# Robust Mesh Data Hiding Based on Irregular Wavelet Transform

William Puech, Meha Hachani, Azza Ouled Zaid

# ROBUST MESH DATA HIDING BASED ON IRREGULAR WAVELET TRANSFORM

*M. Hachani, A. Ouled zaid*

National Engineering School of Tunis
Communication Systems Laboratory
B.P. 37 le Belvédère 1002 Tunis, Tunisia

*W. Puech*

Montpellier University
LIRMM UMR CNRS 5506
161 rue Ada, 34392 Montpollier, France

## ABSTRACT

We present a novel scheme for high-capacity of 3-D triangle meshes. Our proposal can be applied to meshes with arbitrary topology by using irregular wavelet-based analysis. The secret message is inserted in an appropriate resolution level by quantizing the norms of wavelet coefficients vectors. In addition, a re-ordering process is applied as pre-processing in both embedding and extraction stages. Simulation results show that our data hiding framework is robust to common geometric attacks including the operations of the similarity transformations and achieves high data capacity with insignificant visual distortion.

***Index Terms***— 3-D mesh, blind watermarking, quantization, wavelet Transform.

## 1. INTRODUCTION

Data-hiding techniques aim at reliably communicating the largest possible amount of information under given distortion constraints. With the development of 3D hardware, 3D visualization has become much more efficient than ever. This leads to the widespread use of 3D models in various industrial, digital archives, and entertainment applications. Therefore, 3D models are good candidates and rich resources to serve as cover data for hiding other types of digital content [1, 2]. Specifically, data hiding methods are a specific case of high-capacity watermarking. The existing mesh high-capacity watermarking algorithms can fall into two broad categories: spatial domain methods and frequency-domain methods. In the spatial-domain-based methods, the message is embedded directly by modifying the mesh geometry or connectivity. While in a frequency-domain method, the message is inserted by modifying the spectral-like coefficients obtained after a certain mesh transformation. The frequency-domain algorithms are the most favorable since they provide better robustness and imperceptibility. Besides the direct mesh spectral domain, a watermark can also be embedded in the multiresolution domain. In the case of 3-D meshes, multiresolution analysis seems more flexible than the other spectral-like transforms, in sense that it provides different embedding locations that can satisfy different application requirements. Moreover, the mesh multiresolution analysis based on wavelet transform is a very suitable tool for constructing an imperceptible and high-capacity data hiding scheme. Based on the regular wavelet analysis, Kanai et al [3], proposed a non-blind watermarking algorithm for 3-D meshes. Uccheddu *et al.* [4] extends [3] to achieve a blind watermark detection. Recently, Wang et al [5] developed a hierarchical watermarking framework based on wavelet transform of the semiregular meshes. The aforementioned wavelet based watermarking schemes cannot process irregular meshes directly. They can embed the watermark into an irregular mesh by using remeshing that converts an irregular mesh into a semi-regular one. But, the remeshed model cannot be seen as identical to the original, as it corresponds to a different sampling of the underlying 3-D surface. Consequently, the watermark robustness and imperceptibility may be degraded due to this remeshing preprocessing. Using the direct irregular mesh wavelet analysis tool [6], Kim et al [7] proposed a similar correlation-based scheme as in [4] to embed watermark components in bins (groups) of wavelet coefficient vectors (WCVs). Despite its robustness against various geometric attacks, Kim et al. method is penalized by its limited payload capacity and quality degradation.

In the present work, we propose a 3-D mesh data hiding method which is applied in the discrete wavelet transform (DWT) domain. The motivation is to design a blind data hiding system, taking into account the capacity-imperceptibility-robustness-simplicity requirements. For this purpose, we employ an alternative to Quantization Index Modulation (QIM) approach [8] to embed the secret message in the wavelet transform domain. Our proposal can be applied to meshes of arbitrary topological type by using irregular lifting-based wavelet analysis introduced by Valette and Prost [6]. The chosen watermarking primitive is the norm of the wavelet coefficient vector (WCV), at a certain appropriate resolution level. This primitive is invariant to similarity transformations which include translation and rotation. To ensure invariance to similarity transformations, we introduced a re-ordering process as pre-processing on the 3-D model after wavelet analysis.

Experimental results show that despite its simplicity, our approach is characterized by large payloads, robustness to several attack scenarios, and high visual quality reconstruction. The rest of this paper is organized as follows. In Section 2, we explain our data hiding framework in detail. In Section 3, we present the extended version of our embedding scheme to ensure high robustness to similarity transformation attacks. Next, in Section 4 , the particular scenarios simulated are described and the results obtained are presented and discussed. Finally, in Section 5, we conclude and mention potential improvement in future work.

## 2. DESCRIPTION OF THE PROPOSED DATA HIDING FRAMEWORK

In this work, we propose a data hiding scheme based on multiresolution analysis of meshes with arbitrary topology. Our method considers direct replacement of specific wavelet transform coefficients of the cover mesh using quantization watermarking approach. Specifically, the message is embedded by slightly modifying the norms of WCVs associated with a specific resolution level, using non-linear scaling QIM (NLS-QIM) watermark design.

Its is worth mentioning that QIM method is a widely used quantization-based embedding technique for image, audio and video watermarking. Its popularity is, in part, due to its ease of implementation, computational flexibility and large data payloads.

### 2.1. Multiresolution analysis

Here, we briefly recall the principle of the wavelet analysis of irregular meshes, which is proposed by Valette and Prost [6]. First, a mesh $M^0$ is simplified according to an inverse irregular subdivision scheme where each face can be subdivided into four, three, or two faces, or remain unchanged. After the simplification is complete, one can build a hierarchical relationship between the original mesh $M^0$ and the simplified one. Therefore, at a given decomposition level, $j$, the geometry of $M^j$ can be approximated by applying the wavelet decomposition, with two analysis filters. In our work, we used a lifting implementation of the analysis and synthesis filterbanks. The aforementioned process is performed iteratively to finally obtain the coarsest-level irregular mesh $M^J$ and sets of WCVs. By using irregular wavelet analysis scheme, our watermarking method can be applied for both regular and irregular 3D meshes.

### 2.2. Watermark embedding stage

In our work we designed a data hiding scheme, based on dither modulation strategy, meeting these conflicting requirements. For the embedding purpose, we only consider the set$D^j = [d_0, d_1, \ldots, d_{N-1}]^t$ of WCVs associated with the $j^{th}$ intermediate wavelet decomposition level. The Cartesian

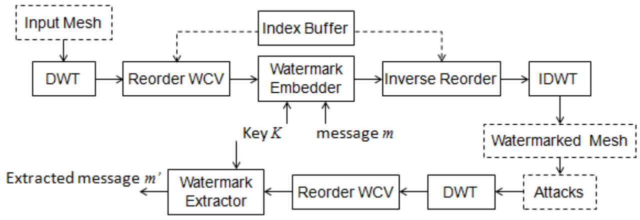


**Fig. 1**. Extended version of our embedding-recovery scheme.

coordinates of the coefficients $d_i$, $i \in \{0, \ldots, N-1\}$ are converted to spherical coordinates $[r_i, \theta_i, \phi_i]^t$ where, $r_i = \|d_i\|$ denotes norm of wavelet coefficient vector $d_i$. Let us consider the watermark message as a binary sequence assigned by $m = \{m_0, \ldots, m_i, \ldots, m_{N-1}\}$, with $m_i \in \{0, 1\}$. These bits are inserted by quantifying the WCV norms $r_i$ according to $\widetilde{r}_i = \lfloor \frac{r_i}{\Delta} \rfloor \times \Delta$. The binary decision results on two modified values $c_0$ and $c_1$ of WCV norm, depending on the quantizer value $\Delta$ and the scaling parameter $\alpha$. When $b_i = 0$ is considered, the binary decision results on the watermarked component $c_0$, given by:

$$\begin{array}{ll} \texttt{if} \;\; r_i \in [\widetilde{r}_i + \alpha, \widetilde{r}_i + \frac{\Delta}{2} - \alpha] & \rightarrow c_0 = r_i; \\ \texttt{if} \;\; r_i \in [\widetilde{r}_i, \widetilde{r}_i + \alpha] & \rightarrow c_0 = \widetilde{r}_i + \alpha; \\ \texttt{if} \;\; r_i > \widetilde{r}_i + \frac{\Delta}{2} - \alpha & \rightarrow c_0 = \widetilde{r}_i + \frac{\Delta}{2} - \alpha; \end{array} \tag{1}$$

Otherwise, if $b_i = 1$ is considered, $c_1$ is given by:

$$\begin{array}{ll} \texttt{if} \;\; r_i \in [\widetilde{r}_i + \frac{\Delta}{2}, \widetilde{r}_i + \frac{\Delta}{2} + \alpha] & \rightarrow c_1 = \widetilde{r}_i + \frac{\Delta}{2} + \alpha; \\ \texttt{if} \;\; r_i \in [\widetilde{r}_i + \frac{\Delta}{2} + \alpha, \widetilde{r}_i + \Delta - \alpha] & \rightarrow c_1 = r_i \\ \texttt{if} \;\; r_i > \widetilde{r}_i + \Delta - \alpha & \rightarrow c_1 = \widetilde{r}_i + \Delta - \alpha; \end{array} \tag{2}$$

This results in the watermarked component $r_i^{'}$, that yields maximum correlation with $r_i$ for a given scaling parameter $\alpha$.

### 2.3. Watermark recovery stage

A given reconstructed WCV norm $r'_i$, positioned in the $j^{th}$ decomposition level, is manipulated using Equation 3 to obtain $Q^0$ and $Q^1$ indices.

$$\begin{array}{l} Q^0 = \begin{cases} \lfloor \frac{r'_i}{\Delta} \rfloor & if \quad r'_i \geq 0 \\ \lfloor \frac{-r'_i}{\Delta} \rfloor & otherwise \end{cases} \\ Q^1 = \begin{cases} \lfloor \frac{r'_i + \frac{\Delta}{2}}{\Delta} \rfloor & if \quad r'_i \geq 0 \\ \lfloor \frac{-r'_i - \frac{\Delta}{2}}{\Delta} \rfloor & otherwise \end{cases} \end{array} . \tag{3}$$

At this step, we measure the distance between $r'_i$ and its approximation, as follows:

$$\begin{array}{rl} \texttt{if} \;\; |r'_i - (Q^1 \times \Delta)| < |r'_i - (Q^0 \times \Delta)| & \rightarrow m_i = 1 \\ \texttt{else} & \rightarrow m_i = 0 \end{array} \tag{4}$$

The capacity of our data hiding approach is equal to the number of wavelet coefficients $N$ in the considered resolution level. In our experiments, the embedding level (EL) corresponds to the third resolution level ($j = 3$).

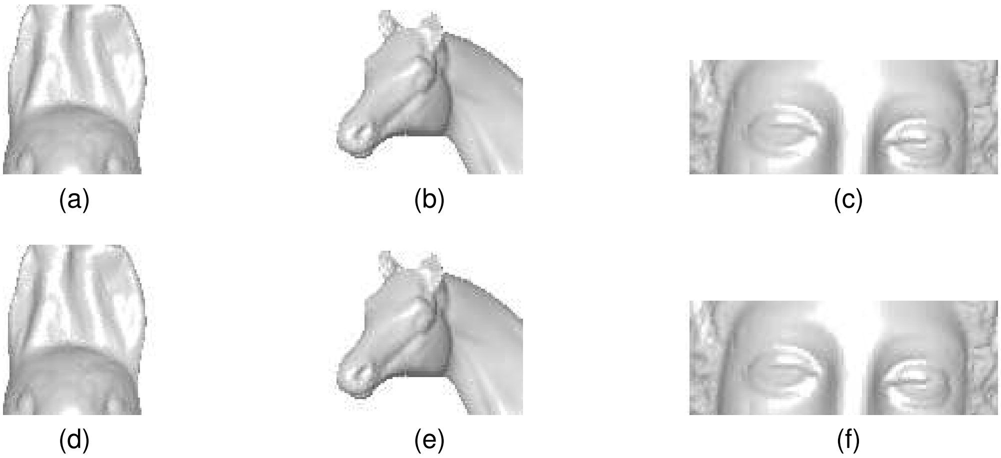


**Fig. 2**. Close-ups of the stego irregular meshes (a) Rabbit, (b) Horse, and (c) Venus. The corresponding close- ups of original meshes are also provided as (d)-(f) for comparison.

## 3. PRE-PROCESSING OF WAVELET COEFFICIENT VECTORS

Despite its efficiency, our embedding method is vulnerable to similarity transformation, which is considered as content-preserving operation. To be invariant to this kind of attack, one just needs to make the watermark synchronization scheme independent of the combinatorial element orders represented in the mesh file. As an extension to our embedding scheme, we propose to establish a robust synchronization (indexing) mechanism. A re-ordering process is applied on the 3-D model after irregular wavelet analysis to achieving the robustness against similarity transformation attack. In more detail, the re-ordering is performed on the N wavelet coefficient vectors localized in the $j^{th}$ resolution level that was selected for embedding purpose. The wavelet coefficients are indexed according to the lengths of their associated edges. First, we sort the edge lengths in ascending order, then we reorder the $N$ WCVs according the the edge length indices. Next the cartesian coordinates of the re-ordered coefficients are converted to spherical coordinates to apply the quantization based embedding as explained in subsection 2.2. It is important to note that the inverse re-ordering of the preprocessed WCVs is required in order to apply the inverse DWT and obtain the watermarked 3-D mesh. The extended version of our data hiding scheme, taking into account the re-ordering strategy, is depicted in a block diagram form as shown in Figure 1.

## 4. EXPERIMENTAL RESULTS

We have tested our data hiding algorithm on several irregular meshes: Venus (100759 vertices), Rabbit (70658 vertices), Horse (112642 vertices), Bunny (34835 vertices), Davidhead (23889 vertices), and Hand (36619 vertices). Concerning the parameter setting, for the QIM based embedding, the quantizer step size $\triangle$ and the $\alpha$ parameter are fixed at 8 and 0.2 respectively, which appear to provide good performances for most of the models. The embedding process was performed on the norms of WCVs at the third resolution level (EL=3). Quality assessment was carried out using two evaluation criteria: maximum root mean square error (MRMS), and mesh structural distortion measure (MSDM). MRMS measures the objective distortion between watermarked and original meshes. A perceptual distance between them is assessed by the MSDM. The robustness is evaluated by the normalized correlation [9] (*corr*) between the extracted watermark binary message and the originally embedded one.

### 4.1. Basic Simulations

Tables 1 and 2 illustrate the baseline evaluations of the proposed H-C data hiding scheme. From the results reported in these tables, it can be seen that, for all the tested meshes, our method introduces relatively high-amplitude deformation while keeping it imperceptible (the induced MSDM is less than 0.078). This point is also confirmed in Figure 2, where three stego and original meshes are depicted. We can hardly observe any visual difference between the cover and stego models. In practice, perceptual distortion measurement is considered more important than the objective distortion measurement since it does not always correctly reflect the visual difference between two meshes. It is worthwhile pointing out that mesh-based applications have very different restrictions on the objective and perceptual distortions induced by the watermark embedding. For example, for the meshes used in digital entertainment, we should ensure that the induced distortion is not annoying to human eyes, while the amount of induced objective distortion is less important. On the other hand, in some mesh applications, such as computer-aided design and medical imaging, it is often required that the induced objec-

**Table 1**. Baseline evaluations of the proposed watermarking framework and Wang's methods for Venus, Rabbit and Horse meshes (in the parentheses are the results of Wang *et al* H-C watermarking method [5]).

| | Venus | Rabbit | Horse |
|---|---|---|---|
| EL | 3 (4) | 3 (4) | 3 (4) |
| Payload (kbits) | 10.909 (7.632) | 3.312(3.18) | 5.28(5.247) |
| MRMS ($10^{-3}$) | 0.2 (0.22) | 0.38 (0.2) | 0.4(0.15) |
| MSDM | 0.04 (0.045) | 0.021 (0.039) | 0.038(0.058) |
| *corr* | 1 (1) | 1 (1) | 1 (1) |

**Table 2**. Baseline evaluations of the proposed data hiding system and Kim's methods for Bunny, Hand and David head meshes (in the parentheses are the results of Kim *et al* method [7]).

| | Bunny | Hand | David head |
|---|---|---|---|
| EL | 3 (1) | 3 (1) | 3 (1) |
| Payload (kbits) | 2.986 (0.265) | 3.26(0.265) | 1.374(0.265) |
| MRMS ($10^{-3}$) | 0.3 (7) | 0.5(9) | 1.4(24) |
| MSDM | 0.024 | 0.045 | 0.078 |
| *corr* | 1 (1) | 1 (1) | 1 (1) |

tive distortion should be very small, while the visual quality of the watermarked model is relatively less important.

The results reported in Tables 1 and 2 also compares the capacity, the embedded message correlation (*corr*), and the MRMS measures provides by our method with those provided by two existing wavelet-based high-capacity watermarking methods (without any robustness consideration): Wang *et al* method [5] (for Venus, Rabbit, Horse meshes), and Kim *et al* method [7] (for Bunny, Davidhead, and Hand meshes). It should be noted that in the case of Wang *et al* watermarking algorithm, the tested mesh is first remeshed to construct a semi-regular mesh before passing through the wavelet decomposition process.

### 4.2. Robustness under various attacks

In this section, we propose to assess the resistance of the embedded message under various attacks, including noise addition, smoothing, and lossy compression. Tables 3, 4 and 5 presents the robustness evaluation results in terms of the normalized correlation $corr$. The distortion induced by attacks is also measured by MRMS and MSDM. The results of the robust watermarking method in [10], based on manifold harmonics transform, are presented in parentheses. It can be seen that with a roughly comparable robustness level, Wang *et al* [10] embedding technique introduces higher geometric and perceptual distortions than our method. Additionally, the watermark message length is relatively short, of about 64 bits, which is still negligible compared to our watermarking approachs capacity. Hence, we can assume that our watermarking scheme has a better trade-off between the robustness, the induced distortion and the capacity payload. However, due to the synchronization issue caused from the wavelet approach of 3-D irregular meshes, we do not consider the resistance under connectivity attacks. To achieve invariance of our data hiding method to this routine operation we extended our embedding technique by integrating the reordering process which was discussed in detail in Section 3. To assess the robustness of our method against the similarity transformation, we applied the operations of translation, rotation and uniform scaling on stego meshes. Tables 6 presents the obtained robustness evaluation results against the considered similarity transformations. It can be observed that experimentally our extended scheme possesses a strong robustness

**Table 3**. Robustness against the random noise addition (in the parentheses are the results of Wang *et al* robust watermarking method [10]).

| Model | Noise | *corr* | MSDM |
|---|---|---|---|
| Venus | 0.05 % | 0.99 (0.85) | 0.097 (0.28) |
| | 0.25 % | 0.99 (0.59) | 0.108 (0.7) |
| | 0.5 % | 0.99 (0.31) | 0.119 (0.83) |
| Rabbit | 0.05 % | 0.99 (0.92) | 0.099 (0.18) |
| | 0.25 % | 0.99 (0.59) | 0.105 (0.6) |
| | 0.5 % | 0.99 (0.31) | 0.111 (0.77) |
| Horse | 0.05 % | 0.99 (0.69) | 0.105 (0.23) |
| | 0.25 % | 0.99 (0.5) | 0.114 (0.64) |
| | 0.5 % | 0.98 (0.08) | 0.12 (0.78) |

**Table 4**. Robustness against the Laplacian smoothing (in the parentheses are the results of Wang *et al* robust watermarking method [10]).

| Model | Iterations | *corr* | MSDM |
|---|---|---|---|
| Venus | 10 | 0.99 (0.74) | 0.101 (0.15) |
| | 30 | 0.99 (0.71) | 0.117 (0.27) |
| | 50 | 0.98 (0.62) | 0.135 (0.34) |
| Rabbit | 10 | 0.99 (0.90) | 0.08 (0.15) |
| | 30 | 0.99 (0.71) | 0.11 (0.26) |
| | 50 | 0.99 (0.45) | 0.142 (0.31) |
| Horse | 10 | 0.99 (0.97) | 0.092 (0.15) |
| | 30 | 0.99 (0.5) | 0.102 (0.23) |
| | 50 | 0.99 (0.35) | 0.135 (0.28) |

**Table 5**. Robustness against coordinate quantization (in the parentheses are the results of Wang *et al* robust watermarking method [10]).

| Model | Quantization | *corr* | MSDM |
|---|---|---|---|
| Venus | 9-bits | 0.99 (0.93) | 0.12 (0.49) |
| | 8-bits | 0.98 (0.70) | 0.26 (0.66) |
| | 7-bits | 0.97 (0.63) | 0.42 (0.79) |
| Rabbit | 9-bits | 0.99 (0.84) | 0.09 (0.44) |
| | 8-bits | 0.99 (0.59) | 0.29 (0.61) |
| | 7-bits | 0.98 (0.05) | 0.53 (0.76) |
| Horse | 9-bits | 0.99 (0.61) | 0.11 (0.44) |
| | 8-bits | 0.97 (0.25) | 0.36 (0.60) |
| | 7-bits | 0.97 (0.17) | 0.51 (0.73) |

**Table 6**. Robustness against similarity transformation (Uniform Scaling $US^{scalingfactor=1.5}$, Translation $T^{(x=0.5,y=0.5,z=1.5)}$ and Rotation $R^{Rotationangle=30^o}$ ).

| | | Models | | |
|---|---|---|---|---|
| | | Venus | Rabbit | Horse |
| $US$ | MSDM | 0.57 | 0.51 | 0.48 |
| | *corr* | 0.992 | 0.995 | 0.993 |
| $T$ | MSDM | 0.48 | 0.14 | 0.19 |
| | *corr* | 1 | 1 | 1 |
| $R$ | MSDM | 0.31 | 0.49 | 0.29 |
| | *corr* | 1 | 1 | 1 |

to this attacks. However, the perceptual distortion is slightly high.

## 5. CONCLUSION

This work proposes a data hiding scheme for 3D meshes. Our embedding framework consists on QIM quantization approach applied to the norms of wavelet coefficient vectors. Simulation results demonstrate that that the proposed method provides significant embedding payloads with the respect to the perceptual/objective watermarked mesh quality. In addition, the embedded message exhibits a high robustness against various kinds of geometric attacks such as lossy compression, random additive noise and Laplacian smoothing. The invariance to similarity transformation was achieved in the irregular wavelet domain by re-ordering the wavelet coefficient vectors.

In our future work, we plan to apply a re-ordering process on the original model before irregular wavelet analysis to achieve the robustness against connectivity re-ordering attacks.

## 6. REFERENCES


[1] K. Wang, G. Lavoué, F. Denis, and A. Baskurt, "A Comprehensive Survey on Three-Dimensional Mesh Watermarking," *IEEE Transactions on Multimedia*, vol. 10, no. 8, pp. 1513–1527, December 2008.

[2] P. Rondao-Alface and B. B. Macq, "From 3d mesh data hiding to 3d shape blind and robust watermarking: A survey," *Lect. Notes Comput. Sci. Trans. Data Hiding Multimedia Security*, vol. 2, pp. 99–115, 2007.

[3] S. Kanai, D. Date, and T. Kishinami, "Digital watermarking for 3d polygon using multiresolution wavelet decomposition," in *Sixth IFIP WG 5.2 GEO-6*, 1998, pp. 296–307.

[4] F. Uccheddu, M. Corsini, and M. Barni, "Wavelet-based blind watermarking of 3d models," in *Workshop on Multimedia and security, ACM Press*, 2004, pp. 143–154.

[5] K. Wang, G. Lavou, F. Denis, and A. Baskurt, "Hierarchical Watermarking of Semiregular Meshes Based on Wavelet Transform," *IEEE Transactions on Information Forensics and Security*, vol. 3, no. 4, pp. 620–634, December 2008.

[6] S. Valette and R. Prost, "Multiresolution analysis of irregular surface meshes," *IEEE Transactions on Visualization and Computer Graphics*, vol. 10, pp. 113–122, 2004.

[7] M.S. Kim, S. Valette, H.Y. Jung, and R. Prost, "Watermarking of 3D irregular meshes based on wavelet multiresolution analysis," in *International Workshop on Digital Watermarking (IWDW'05)*, 2005, pp. 313–324.

[8] B. Chen and G. W. Wornell, "Quantization index modulation, a class of provably good methods for digital watermarking and information embedding," *IEEE Transactions on Information Theory*, vol. 47, no. 4, pp. 1423–1443, 2001.

[9] I.J. Cox, M.L. Miller, J.A. Bloom, J. Fridrich, and T. Kalker, *Digital Watermarking and Steganography*, Morgan Kaufmann Publishers Inc., 2007.

[10] K. Wang, M. Luo, A.G Bors, and F. Denis, "Blind and robust mesh watermarking using manifold harmonics," in *IEEE International Conference on Image Processing (ICIP)*, 2009, pp. 3657–3660.